Available online at www.sciencedirect.com
ScienceDirect
Ceramics International 38 (2012) 527–533
CERAMICS INTERNATIONAL
www.elsevier.com/locate/ceramint

Mechanical properties and electrical conductivity in a carbon nanotube reinforced silicon nitride composite

A. Kovalčíková [a,*], Cs. Balázsi [b], J. Dusza [a], O. Tapasztó [b]

[a] Institute of Materials Research, Slovak Academy of Sciences, Watsonova 47, 040 01 Košice, Slovak Republic
[b] Ceramics and Nanocomposites Department, Research Institute for Technical Physics and Materials Science, Konkoly-Thege ut 29-33, 1121 Budapest, Hungary

Received 24 May 2011; received in revised form 7 July 2011; accepted 21 July 2011
Available online 28th July 2011

Abstract

The influence of carbon nanotubes (CNTs) addition on basic mechanical, thermal and electrical properties of the multiwall carbon nanotube (MWCNT) reinforced silicon nitride composites has been investigated. Silicon nitride based composites with different amounts (1 or 3 wt%) of carbon nanotubes have been prepared by hot isostatic pressing. The fracture toughness was measured by indentation fracture and indentation strength methods and the thermal shock resistance by indentation method. The hardness values decreased from 16.2 to 10.1 GPa and the fracture toughness slightly decreased by CNTs addition from 6.3 to 5.9 MPa $m^{1/2}$. The addition of 1 wt% CNTs enhanced the thermal shock resistance of the composite, however by the increased CNTs addition to 3 wt% the thermal shock resistance decreased. The electrical conductivity was significantly improved by CNTs addition (2 S/m in 3% Si_3N_4/CNT nanocomposite).

Keywords: C. Electrical conductivity; C. Mechanical properties; C. Thermal shock resistance; Si_3N_4–CNT composites

1. Introduction

Silicon nitride has very good combination of mechanical, physical, and chemical properties. The strength, hardness, and toughness at room and elevated temperatures make it suitable for use in several structural applications [1]. To obtain superior mechanical properties, a fine-grained microstructure with elongated beta grains is preferred. These in situ grown beta silicon nitride grains can significantly improve the fracture toughness over monolithic ceramics, producing self-reinforced silicon nitrides [2]. Ex situ toughening of silicon nitrides is also accomplished with the addition of fibers such as SiC and carbon [3,4].

Carbon nanotubes (CNTs) offer new possibilities to improve the functional and mechanical properties of advanced ceramics thanks to their small size, large aspect ratio, low mass and excellent mechanical, electrical and thermal properties [5,6]. For high-temperature applications, the high thermal conductivity of CNTs suggests that their incorporation, even at low volume fraction, might provide the thermal transport needed to reduce material operating temperatures and improve thermal shock resistance [7]. Such composites may find applications in catalyst supports, hydrogen storage, electrodes for fuel cells, supercapacitors, and ultrafiltration membranes. During the last decade new ceramic/carbon nanotube composites have been developed and a number of authors have reported improved mechanical and functional properties in the case of ceramic/CNT composites compared to the monolithic material [8–16]. Three main problems have been recognized during these investigations: dispersion of the CNTs in the matrix, densification of the composites and degradation of the CNTs [17–20].

An increase of the fracture toughness and of electrical conductivity has been achieved in CNTs reinforced alumina matrix composites, but only modest improvements of electrical and mechanical properties were found in carbon nanotube silicon carbide-, polymer-, metal oxide matrix composites [21–24]. CNT-CMC materials have demonstrated significant enhancements in electrical conductivity at relatively low CNT volume fractions. It was reported that CNT-dispersed Al_2O_3 fabricated by the spark plasma sintering (SPS) method, which is one of the densification techniques at low

* Corresponding author. Tel.: +421 55 792 2463; fax: +421 55 792 2408.
E-mail address: akovalcikova@imr.saske.sk (A. Kovalčíková).

0272-8842/$36.00
doi:10.1016/j.ceramint.2011.07.038

temperatures, had extremely high fracture toughness, because of the bridging effect of CNTs [25]. Furthermore, the strength of these materials is degraded by CNT dispersion due to insufficient densification, although CNTs should improve the mechanical properties. CNT dispersed silicon nitride composites have been made by Balázsi et al. [26] with improvements in strength, stiffness, and toughness. Tatami et al. [9] developed CNT dispersed Si_3N_4 ceramics with high density, electrical conductivity, and superior mechanical properties by using novel sintering aids (Y_2O_3–Al_2O_3–TiN–AlN).

Most work on CNT-CMCs has focused on the measurement of toughness using the indentation/crack length technique but most results for toughening have been disappointing. Data has shown very little or no increase in toughening upon introduction of CNTs – either single- or multi-walled – into various ceramic matrices [21,27,28]. Toughening has been obtained through the toughening mechanisms e.g. crack bridging by CNTs, crack deflection at CNT/matrix interface and nanotube pull-out on the fracture surface [1,29]. The mechanical properties strongly depend on the type of nanotubes, as well as nanotube/matrix interactions [26].

Recently, different investigations have been focused on the study of the grain boundaries in different CNTs/CNFs reinforced ceramic composites [30–33]. Vasiliev [30,31] based on the results of transmission electron microscopy (TEM) and high-resolution transmission electron microscopy (HREM), presented a new way of perceiving grain boundaries in alumina/SWCNTs composite. Balázsi [32] investigated the interface between the beta-Si_3N_4 crystallites and MWCNTs by TEM and HREM in the composites based on silicon nitride and reinforced by 1 and 3 wt% of MWCNTs. Kothari et al. [33] during investigation of the effect of MWCNTs and dense as received and heat treated CNFs on the reinforcement in amorphous silicon nitride coatings, found that the heat treatment of CNFs changed the character of the CNT/matrix interface and increased the pull-out. Significantly longer pull-out was found however in the case of MWCNTs.

However, only few researchers [11] have been concerned with thermal properties of carbon nanotube composites in ceramic systems. The thermal shock resistance of brittle materials generally depends on a number of thermal and mechanical properties mainly thermal expansion coefficient, thermal conductivity, thermal diffusivity, Young's modulus, fracture toughness, strength, heat transfer coefficient, specimen size and duration of the thermal shock. Several thermal shock parameters have been defined to relate these materials to their thermal resistance, considering the crack initiation (R parameter) and crack propagation (R'''' parameter) conditions, respectively. They are defined as following [34]:

$$R = \frac{\sigma_c(1-\upsilon)}{\alpha E} = \Delta T_c \quad (1)$$

$$R'''' = \left(\frac{K_{IC}}{\sigma_r}\right)^2 (1+\nu) \quad (2)$$

where σ is the tensile strength, E the Young's modulus, α the coefficient of thermal expansion, K_{IC} is fracture toughness and ν is the Poisson's ratio.

Higher values of R represent greater resistance to fracture initiation during quenching and higher values of R'''' indicate less crack propagation once the critical temperature drop ΔT_c, necessary to initiate fracture, is exceeded.

In convectional testing thermal shock resistance is quantified by measuring of residual strength of polished specimens after quenching. This standardized method requires a large number of prepared (at least 30 samples) and it cannot allow multiple shock measurements. For these reasons an alternative indentation-quench method has been developed by Andersson and Rowcliffe [35]. In this technique, the thermal shock resistance is measured by studying the propagation of median/radial cracks around a Vickers indentation after single or repeated quenching. The critical temperature difference $\Delta T_{c\ ind}$, of the material can be defined with reference to the number of propagating cracks and the amount of crack extension.

The thermal shock resistance of Si_3N_4/CNTs composites has not yet been reported, but many authors have studied thermal shock resistance of different ceramic materials by water quenching or indentation tests (silicon nitride, silicon carbide, β-sialons, alumina/silicon carbide nanocomposites, etc.) [36–40].

The aim of the present contribution is to investigate the influence of the carbon nanotubes (CNTs) addition on the hardness, fracture toughness, thermal shock resistance and electrical conductivity of multiwall carbon nanotube (MWNT) reinforced silicon nitride composites.

2. Experimental materials and methods

2.1. Starting material and experimental setup

Some details about composition of the starting powder mixtures and preparation can be seen in Table 1. Si_3N_4 (Ube, SN-ESP), Al_2O_3 (Alcoa, A16) and Y_2O_3 (H.C. Starck, grade C)

Table 1
Starting compositions and preparation conditions of sintered samples.

Samples	Starting powders (wt%)			CNT (MWNT) (wt%)	Ball milling (wt%)	Ultrasonic agitation (wt%)	Sintering conditions		
	Si_3N_4	Al_2O_3	Y_2O_3				Temp. (°C)	Holding time	Pressure (MPa)
SN	90	4	6	–	3 h	–	1700	3 h	20
SN-CNT1	90	4	6	1	3 h	3 h (mixture + MWCNT)	1700	3 h	20
SN-CNT2	90	4	6	3	3 h	3 h (mixture + MWCNT)	1700	3 h	20

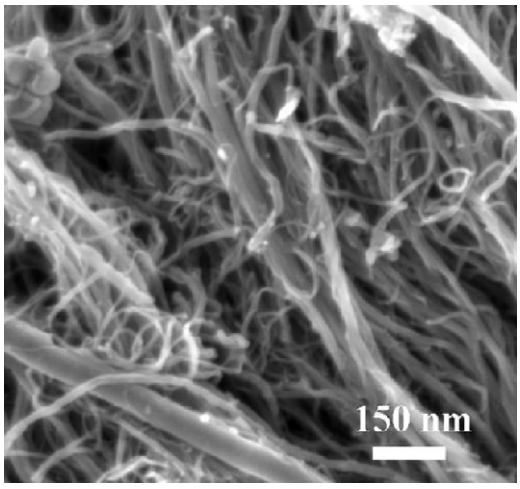

Fig. 1. The morphology of multiwall carbon nanotubes (MWCNTs).

were used as starting powders. Different amounts of CNTs (multiwall carbon nanotubes, produced as described elsewhere [41]) were added in addition to batches (1 and 3 wt%). The morphology of multiwall carbon nanotubes (MWCNTs) is shown by SEM (Fig. 1). The SEM is revealing the non-homogeneous dimensions of MWCNTs prepared by chemical vapour deposition (CVD). The MWCNTs are 10–70 nm in diameter and 8–10 μm in length. The powder mixtures together with the added CNTs were milled in ethanol in a planetary type alumina ball mill for 3 h. The powder mixtures and CNTs were introduced in an ethanol bath and sonicated together. After sonication surfactants (polyethyleneglycol, PEG) were added to the powder mixture. The batches were dried and sieved. Green samples were obtained by dry pressing at 220 MPa. Before sintering an oxidation was applied at very low heating rates up to 400 °C, to eliminate the PEG from samples. The samples without CNT were fabricated in the same manner, and their properties were evaluated. Hot isostatic pressing was performed at 1700 °C in high purity nitrogen by a two-step sinter-HIP method using BN embedding powder. The heating rate was not exceeding 25 °C/min. The gas pressure was 20 MPa. The dimensions of the as-sintered specimens were 3.5 mm × 5 mm × 50 mm. All surfaces of the samples were finely ground and polished on a diamond wheel, and the edges were chamfered.

2.2. Density, microstructure and mechanical properties

The density of the sintered materials was measured by Archimedes method with distilled water. The fracture surfaces were studied using an SEM (JEOL JSM-7000F). Microfractography was used to analyse the fracture lines and surfaces of the specimens to study the fracture micromechanisms in the monolithic material and in the composites.

Hardness was determined by Vickers indentation (hardness testers LECO 700AT) and calculated according to the equation [42]:

$$H = 1.8544\left(\frac{P}{d^2}\right) \tag{3}$$

where d is the indentation diagonal and P the indentation load.

The fracture toughness was measured by Indentation strength (IS) and Indentation fracture (IF) method. Vickers indentations were introduced into the specimens with dimensions of 3 mm × 4 mm × 45 mm that were then loaded in four-point-flexure mode (inner span of 20 mm and outer span of 40 mm). The specimens were tested with the crosshead speed of 0.5 mm/min at ambient temperature and atmosphere. The strength (σ_f) value has been determined and the fracture toughness was calculated using the equation [43]:

$$K_{IC} = 0.88(\sigma_f P_i^{1/3})^{3/4} \tag{4}$$

The IF values was determined by the measurement of the crack lengths created by Vicker's indentations at the load of 98 N. Fracture toughness was calculated using a formula valid for semi-circular crack systems as proposed by Shetty et al. [44]:

$$K_{IC} = 0.0899\left(\frac{HP}{4l}\right)^{0.5} \tag{5}$$

where H is the hardness, P is the indentation load and $l = c - a$ is the length of the indentation crack (c – half length of the radial crack, a – half length of diagonal).

For the investigation of thermal shock resistance the indentation-quench method was used. Thermal shock tests were conducted on bars with dimension of 3 mm × 4 mm × 25 mm. They were ground and polished with final diamond paste of 1 μm. All indentations were made with a 98.1 N load to obtain the pre-cracks approximately in the same length. Each indent generated four cracks, so that 12 cracks were made on one sample. Measurements were performed on three samples of each material.

The length of the cracks was measured using optical microscopy. After the indentation the samples were heated in a vertical tube furnace in air to the required temperature and held there for 25 min. Then the specimens were rapidly immersed into a ~20 °C water bath. Final radial crack lengths were then measured with optical microscope. The procedure was repeated at increasing quenching temperatures ΔT, up to the critical value of ΔT_c at which radial crack became unstable and the specimen failed.

The electrical conductivity of monolithic and composite materials was measured at ambient temperature using a two-point probe setup, carried out on a precision impedance analyzer Agilent 4294A. Specimens with the dimension of 3 mm × 4 mm × 10 mm were cut from the centre of the hot pressed samples for these measurements. As the probes two copper electrodes with area of 1 mm^2 were applied on opposite faces of the experimental discs. Measurements were carried out at frequency range from 40 Hz to 40 kHz.

3. Results and discussion

3.1. Microstructure

Morphological observation of fracture surfaces of HIP samples is presented in Fig. 2. The microstructure of sintered

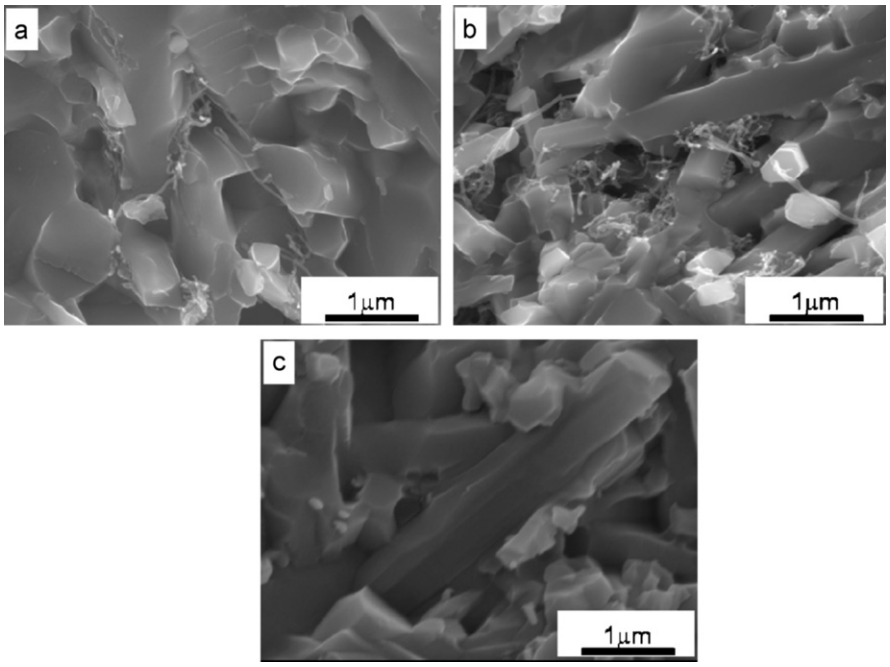

Fig. 2. Fracture surfaces of HIP samples: (a) CNT/Si_3N_4 composites with 1%CNT, (b) CNT/Si_3N_4 composites with 3%CNT, (c) Si_3N_4 reference sample.

MWCNT composites consisted mainly of β-Si_3N_4 grains (several micro meters in length) and nanotubes. The CNTs are located mainly in the inter-granular positions and they have a good contact to the surface of silicon nitride grains. As can be observed, the dispersion of MWNTs is still far from optimum, in most of the cases they are in interconnected groups. Agglomeration of bundles of MWCNTs between the silicon nitride boundaries inhibits the densification of composites. For this reason, CNT added samples had significantly larger porosity than reference sample and the reinforcement processes (e.g. pullouts, crack bridging) are still not enough for a significant strengthening. However, separated MWNTs can also be observed.

3.2. Hardness and fracture toughness

The density and basic mechanical properties are summarized in Table 2. High density monolithic ceramic and nanocomposites have been achieved. The reference sample without any nanotube addition has the highest degree of densification. An addition of MWCNTs decreases the density from 3.14 to 2.65 g cm^{-3}. The hardness of the composites is lower compared to the hardness of the monolithic material. The Vickers hardness of the composites significantly decreased with increasing content of the MWCNTs. The hardness for the silicon nitride/CNTs composites was 13.3 GPa and 10.1 GPa respectively. Tatami et al. [9] developed CNT (1.8 wt%) dispersed Si_3N_4 ceramics with hardness of 14.3 GPa. The lower hardness of the composite compared to the monolithic material is mainly dependent on the residual porosity that remains in the material after the sintering, similar to that observed in other investigation [15]. Together with the porosity, the clusters of the CNFs/CNTs are characteristic processing defects present in our material and presented in all of the work dealing with similar composites. This indicates the still present difficulties at the preparation of defect free carbon nanotubes or carbon nanofibers reinforced ceramic composites but also the potential for the improvement of their functional and mechanical properties.

Si_3N_4 samples have an indentation fracture toughness of 6.2–6.3 MPa $m^{1/2}$. The fracture toughness of the composites with 1 wt% and 3 wt% CNT is 6.0 and 5.9 MPa $m^{1/2}$, respectively. The variation of fracture toughness with indentation load (*R*-curve-like behaviour) is estimated by changing the indentation load over a range 9.81–98.1 N. Silicon nitride shows a characteristic toughening (*R*-curve) behaviour with an increased crack growth resistance connected with increased crack length. In the case of composites, classic *R* curve behaviour is not evident, Fig. 3. However, Pasupuleti et al. [1] achieved improved fracture toughness of Si_3N_4/CNT connected with self-reinforcement effect. They also showed *R*-curve behaviour for composites and crack-path deflection as main toughening mechanisms. Xia et al. [29] reported that the

Table 2
Physical and mechanical properties of the investigated materials.

Samples	Density (g cm^{-3})	HV1 (GPa)	$K_{IC,ind}$ (MPa $m^{1/2}$)	IS (MPa $m^{1/2}$)	Electrical cond. (S/m)	R_{exp} (°C)
SN	3.28	16.2 ± 0.5	6.3 ± 0.4	6.7 ± 0.2	–	780
SN-CNT1	3.14	13.3 ± 0.6	6.0 ± 0.4	5.7 ± 0.3	257×10^{-12}	870
SN-CNT2	2.65	10.1 ± 0.6	5.9 ± 0.3	4.4 ± 0.4	1.98	600

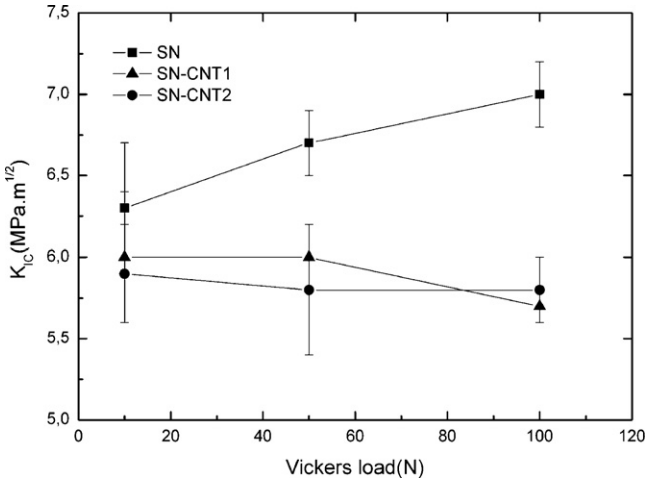

Fig. 3. R-curve like behaviour of sintered materials.

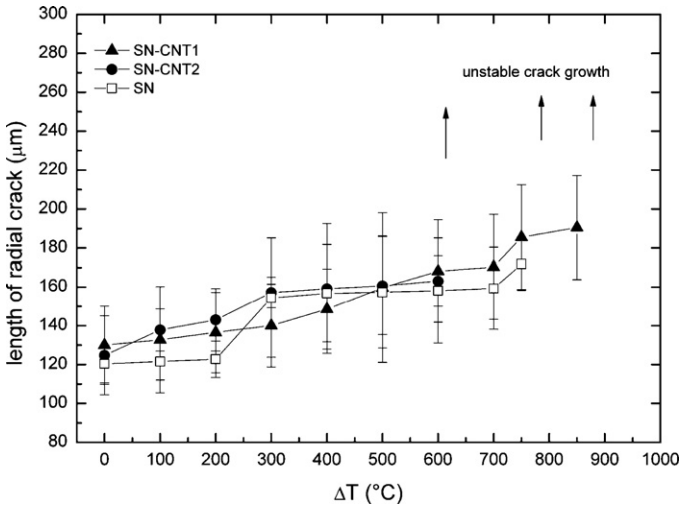

Fig. 4. Crack propagation at thermal shock tests; the temperature difference at which unstable cracking begins are marked by arrows.

predominant toughening mechanisms in Si_3N_4/CNT composites were pullout and crack deflection. In our case these toughening mechanisms are not present in the composites from two reasons. The first, the main reason is the relatively high porosity mainly in the case of composite with 3 wt% of CNTs. This porosity eliminates the possibility of toughening by CNTs moreover limit the toughening by the elongated Si_3N_4 grains, too. The second reason is the non uniform distribution of CNTs, the effect of this will be visible in the case of full dense materials only.

3.3. Thermal shock resistance

Petterson et al. [38] in his study mentioned that the material with better thermal shock resistance can absorb the residual stress at the higher loads better than the poorer material. When too high a load is used (the initial cracks are too long) the crack growth depends both on the relaxation of residual stress in the material and on the thermal shock. A good choice seems to be an initial crack length of 100 ± 10 μm for testing of Si_3N_4 based ceramics. The initial cracks size for silicon nitrides samples were ≈120 μm at indentation load 98.1 N. The dependence of radial crack growth on temperature for tested materials is plotted in Fig. 4. There are visible three different areas which characterize the crack evolution after quenching: (a) an initial radial cracks growing slightly with increasing ΔT (area to $\Delta T \sim 200$ °C); (b) a radial crack growing stable extension (area from $\Delta T \sim 200$ °C to $\Delta T \sim 700$ °C); (c) a radial crack growing unstable extension and the specimens failed. A critical temperatures ΔT_c when the Si_3N_4 failed is ∼780 °C.

In the case of Si_3N_4/CNT reinforced composites the initial crack length was above 125–130 μm at indentation load 98.1 N. Again are visible different areas which characterize the crack evolution after quenching: (a) an initial radial cracks growing slightly with increasing ΔT (area to $\Delta T \sim 250$ °C for SN-CNT1, to $\Delta T \sim 200$ °C for SN-CNT2); (b) a radial crack growing stable extension (area from $\Delta T \sim 250$ °C to $\Delta T \sim 700$ °C for SN-CNT1, from $\Delta T \sim 200$ °C to $\Delta T \sim 600$ °C for SN-CNT2; (c) a radial crack growing unstable extension and the specimens failed ($\Delta T_c \sim 870$ °C for SN-CNT1 and $\Delta T_c \sim 620$ °C for SN-CNT2).

With increasing the carbon nanotube content a decrease of thermal shock resistance has been observed. Thermal shock resistance can be improved by the increased flexural strength and fracture toughness and by decreased Young's modulus and coefficient of thermal expansion. Materials with very strong *R*-curve behaviour are probably most suitable for thermal shock applications. Because fracture toughness for Si_3N_4/CNT is not differ significantly from the values of monolithic silicon nitride (materials with *R*-curve behaviour enhanced thermal shock resistance), the reason for lower thermal shock resistance could be degraded strength values by CNT dispersions due to insufficient densification [10]. The other possible reason is a difference in thermal properties of the materials – different thermal expansion coefficients of silicon nitride (3×10^{-6} K^{-1}) and MWCNTs ($1.6–2.6 \times 10^{-5}$ K^{-1}).

Microfractographic observation of thermally shocked specimens with Vickers indentation showed wheel defined radial crack pattern. The propagation of Vickers indentation crack of SN-CNT1 before thermal shock is shown in Fig. 5a, after thermal shock at $\Delta T = 870$ °C in Fig. 5b. These cracks increased in size with increasing temperature, but always reached instability first in the longitudinal direction (i.e. crack aligned parallel to the specimen length). This indicates a slightly higher tension in the transverse direction, consistent with some edge effect in the thermal transfer process (via r_0 in the Biot coefficient) [37].

3.4. Electrical conductivity

It is well known that silicon nitride is an insulator with extremely low electrical conductivity. It was found that electrical conductivity increase with CNT content. As shown in Table 2, the room temperature electrical conductivity is about 2 S/m in 3 wt% Si_3N_4/CNT nanocomposite while 1 wt% Si_3N_4/CNT is still insulator. In a previous study we demonstrated an increase in thermal conductivity for carbon nanotube added

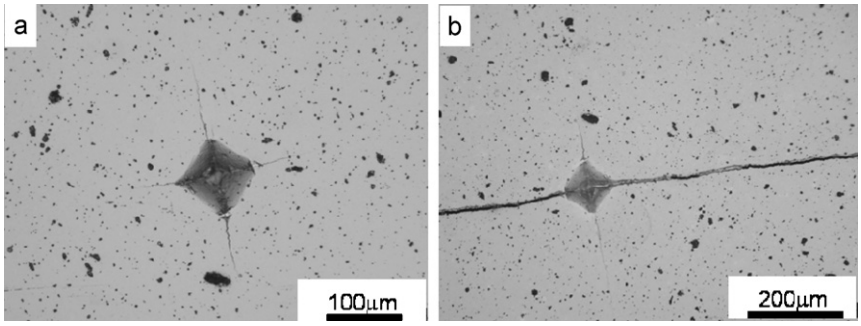

Fig. 5. Vickers indentation crack of SN-CNT1, (a) before thermal shock; (b) after thermal shock ($\Delta T = 870$ °C).

Si_3N_4 ceramic nanocomposites using MWCNTs as reinforcements [45]. The SN-CNT2 nanocomposites showed a 4% increase in thermal conductivity at 200 °C compared to SN sample. In a recent work by Corral et al. [46] demonstrated that singlewall carbon nanotubes (SWCNTs) can be used to effectively tailor both electrical and thermal properties of silicon nitride. However, as the nanocomposite room temperature electrical conductivity increases with increasing SWCNT addition, the opposite trend is observed for thermal conductivity properties. They suggested that several factors should be taken account for the lower thermal conductivity. One factor is the higher porosity of composites with MWCNT addition. The other possible factors can be the CNT induced phonon scattering points and the interface effects between CNTs and matrix all reducing the thermal conductivity. Tatami et al. [9] achieved the electrical conductivity of 2.8 S/m in the silicon nitride sample with 1.8 wt% of CNT prepared by GPS technique, 79 S/m in the sample prepared by HP and about 30 S/m for composite fabricated by HIP. Balázsi et al. [47] investigated the influence of the carbon nanotube (CNT), black-carbon (BC) and graphite (GR) addition on the electrical conductivity of Si_3N_4. It was found that the size and shape of the mixed graphite additives resulted in a very limited graphite grain connection in the matrix, which resulted in the lowest electrical conductivity of the composite prepared using this additive. The composite with the highest conductivity produced with carbon black additions thanks to their nano size producing bunchy, chain cluster forms in the pores and on the surface of the matrix grains. In the case of 5% CNT addition an electrical conductivity in the range of 4.32–12 S/m was achieved.

Zhan et al. [20] measured the conductivity on alumina-based material and obtained 15 S/m at about 15% CNT. The thermoelectric properties of 10 vol.% single-wall carbon nanotube/3Y-TZP nanocomposite produced by SPS have been studied by Zhan and Mukherjee [11]. According to these results, the electrical conductivity decreased from approximately 500 S/m to approximately 200 S/m when the temperature increased from room temperature to 550 K. A further increase of the testing temperature resulted in a slight increase of electrical conductivity. Shi and Liang [48] studied the effect of the MWCNT addition on the electrical and dielectric properties of MWCNT/3Y-TZP composite prepared by SPS. They found a very strong influence of the CNTs addition on the electrical conductivity of the composite in the range of addition from 1 to 2 wt% of CNTs. MWCNT/3Y-TZP composites have been prepared by pressureless sintering + HIP by Ukai et al. [16]. For the materials with weight % of CNTs from 0.25 to 1.0 the electrical conductivity was found to be in the interval from 5 to 60 S/m.

4. Conclusions

In this study the carbon nanotube dispersed silicon nitride ceramics with high density, good mechanical properties, higher electrical conductivity and comparable thermal shock resistance to silicon nitride ceramics was prepared.

The hardness values decreased with addition of MWCNTs and the fracture toughness is comparable with fracture toughness of silicon nitride. With increasing the carbon nanotube content a decrease of thermal shock resistance has been observed. Because fracture toughness for Si_3N_4/CNT is not differ significantly from the values of monolithic silicon nitride (materials with strong *R*-curve behaviour are probably most suitable for thermal shock applications), the reason for lower thermal shock resistance could be degraded strength values by CNT dispersions due to insufficient densification. The room temperature electrical conductivity is about 2 S/m in 3 wt% Si_3N_4/CNT nanocomposite while 1 wt% Si_3N_4/CNT is still insulator.

Acknowledgements

This work was realized within the frame of the project ‘‘Centre of Excellence of Advanced Materials with Nano- and Submicron-Structure’’, which is supported by the Operational Program ‘‘Research and Development’’ financed through European Regional Development Fund and by the Slovak Government through project APVV LPP 0203-07.

References

[1] S. Pasupuleti, R. Peddetti, S. Santhanam, K.-P. Jen, Z.N. Wing, M. Hecht, J.P. Halloran, Toughening behavior in a carbon nanotube reinforced silicon nitride composite, Mater. Sci. Eng. A 491 (2008) 224–229.
[2] H. Imamura, K. Hirao, M. Brito, M. Toriyama, S. Kanzaki, Further improvement in mechanical properties of highly anisotropic silicon nitride ceramics, J. Am. Ceram. Soc. 83 (2000) 495–500.
[3] C. Wang, Y. Huang, Z. Xie, Improved resistance to damage of silicon carbide-whisker-reinforced silicon nitride-matrix composites by whisker-oriented alignment, J. Am. Ceram. Soc. 84 (2001) 161–164.

[4] H. Hyuga, M.I. Jones, K. Hirao, Y. Yamauchi, Friction and wear properties of Si_3N_4/carbon fiber composites with aligned microstructure, J. Am. Ceram. Soc. 88 (2005) 1239–1243.
[5] S. Iijima, Helical microtubules of graphitic carbon, Nature 354 (1991) 56–58.
[6] A. Merkoci, Carbon nanotubes in analytical sciences, Microchim. Acta 152 (2006) 157–174.
[7] W.A. Curtin, B.W. Sheldon, CNT-reinforced ceramics and materials, Mater. Today (2004) 44–49.
[8] X. Wang, N.P. Padture, H. Tanaka, Contact-damage-resistant ceramic/single-wall carbon nanotubes and ceramic/graphite composites, Nat. Mater. 3 (2004) 539–544.
[9] J. Tatami, T. Katashima, K. Komeya, T. Meguro, T. Wakihara, Electrically conductive CNT-dispersed silicon nitride ceramics, J. Am. Ceram. Soc. 88 (2005) 2889–2895.
[10] Cs. Balázsi, Z. Kónya, F. Wéber, L.P. Biró, P. Arató, Preparation and characterization of carbon nanotube reinforced silicon nitride composites, Mater. Sci. Eng. C23 (2003) 1133–1138.
[11] G.D. Zhan, A.K. Mukherjee, Carbon nanotube reinforced alumina based ceramics with novel mechanical, electrical and thermal properties, J. Appl. Ceram. Technol. 1 (2) (2004) 161–171.
[12] G.D. Zhan, J.D. Kuntz, J.E. Garay, A.K. Mukherjee, P. Zhu, K. Koumoto, Thermoelectric properties of carbon nanotube/ceramic nanocomposites, Scripta Mater. 54 (2006) 77–82.
[13] Ch. Laurent, A. Peigney, O. Dumortier, A. Rousset, Carbon nanotubes–Fe–alumina nanocomposites. Part II: microstructure and mechanical properties of the hot-pressed composites, J. Eur. Ceram. Soc. 18 (1998) 2005–2013.
[14] A. Peigney, S. Rul, F. Lefevre-Schick, C. Laurent, Densification during hot-pressing of carbon nanotube-metal-magnesium aluminate spinel nanocomposites, J. Eur. Ceram. Soc. 27 (2007) 2183–2193.
[15] J. Sun, L. Gao, M. Iwasa, T. Nakayama, K. Niihara, Failure investigation of carbon nanotube/3Y-TZP nanocomposites, Ceram. Int. 31 (2005) 1131–1134.
[16] T. Ukai, T. Sekino, A. Hirvonen, N. Tanaka, T. Kusunose, T. Nakayama, K. Niihara, Preparation and electrical properties of carbon nanotubes dispersed zirconia nanocomposites, Key Eng. Mater. 317–318 (2006) 661–664.
[17] F. Inam, H. Yan, M.J. Reece, T. Peijs, Dimethylformamide: an effective dispersant for making ceramic-carbon nanotube composites, Nanotechnology 19 (2008) 195710.
[18] J.W. An, D.H. You, D.S. Lim, Tribological properties of hot-pressed alumina–CNT composites, Wear 255 (2003) 677–681.
[19] Y.Q. Liu, L. Gao, A study of the electrical properties nanotube-$NiFe_2O_4$ composites: effect of the surface treatment of the carbon nanotubes, Carbon 43 (2005) 47–52.
[20] G.D. Zhan, J.D. Kuntz, J.E. Garay, A.K. Mukherjee, Electrical properties of nanoceramics reinforced with ropes of single-walled carbon nanotubes, Appl. Phys. Lett. 83 (2003) 1228–1230.
[21] E. Flahaut, A. Peigney, Ch. Laurent, Ch. Marliere, F. Chastel, A. Rousset, Carbon nanotube–metal-oxide nanocomposites: microstructure, electrical conductivity and mechanical properties, Acta Mater. 48 (2000) 3803–3812.
[22] H. Dai, Carbon nanotubes: opportunities and challenges, Surf. Sci. 500 (2002) 218–241.
[23] H.D. Wagner, Nanotube-polymer adhesion: a mechanics approach, Chem. Phys. Lett. 361 (2002) 57–61.
[24] S.J. Park, M.K. Seo, H.B. Shim, Effect of fiber shapes on physical characteristics of non-circular carbon fibers-reinforced composites, Mater. Sci. Eng. A 352 (2003) 34–39.
[25] G.-D. Zhan, J.D. Kuntz, J. Wan, A.K. Mukherjee, Single-wall carbon nanotube as attractive toughening agent in alumina based nanocomposites, Nat. Mater. 2 (2003) 38–42.
[26] Cs. Balázsi, F. Wéber, Zs. Köver, Z. Shen, Z. Kónya, Zs. Kasztovszky, Z. Vértesy, L.P. Biró, I. Kiricsi, P. Arató, Application of carbon nanotubes to silicon nitride matrix reinforcements, Curr. Appl. Phys. 6 (2006) 124–130.
[27] R.W. Siegel, S.K. Chang, B.J. Ash, J. Stone, P.M. Ajayan, R.W. Doremus, L.S. Schadler, Scripta Mater. 44 (2001) 2061–2064.
[28] A. Peigney, Aligned carbon nanotubes in ceramic-matrix nanocomposites prepared by high-temperature extrusion, Chem. Phys. Lett. 352 (2002) 20–25.
[29] Z. Xia, L. Riester, W.A. Curtin, H. Li, B.W. Sheldon, J. Liang, B. Chang, J.M. Xu, Direct observation of toughening mechanisms in carbon nanotube ceramic matrix composites, Acta Mater. 52 (2004) 931–944.
[30] L.A. Vasiliev, R. Poyato, P.N. Padture, Single-wall carbon nanotubes at ceramic grain boundaries, Scripta Mater. 56 (2007) 461–463.
[31] R. Poyato, L.A. Vasiliev, P.N. Padture, H. Tanaka, T. Nishimura, Aqueous colloidal processing of single-wall carbon nanotubes and their composites with ceramics, Nanotechnology 17 (2006) 1770.
[32] Cs. Balázsi, K. Sedláčková, Zs. Czigány, Structural characterization of Si_3N_4–carbon nanotube interfaces by transmission electron microscopy, Compos. Sci. Technol. 68 (2008) 1596–1599.
[33] K.A. Kothari, K. Jian, J. Rankin, B.W. Sheldon, Comparison between carbon nanotube and carbon nanofiber reinforcements in amorphous silicon nitride coatings, J. Am. Ceram. Soc. 91 (2008) 2743–2746.
[34] D.P.H. Hasselman, Thermal stress resistance parameters for brittle refractory ceramics: a compendium, Am. Ceram. Soc. Bull. 49 (1970) 1033–1037.
[35] T. Andersson, D.J. Rowcliffe, Indentation thermal shock test for ceramics, J. Am. Ceram. Soc. 79 (1996) 1509–1514.
[36] M. Kalantar, G. Fantozzi, Thermo-mechanical properties of ceramics: resistance to initiation and propagation of crack in high temperature, Mater. Sci. Eng. A 472 (2008) 273–280.
[37] S.K. Lee, J.D. Moretti, M.J. Readey, B.R. Lawn, Thermal shock resistance of silicon nitride using an indentation-quench test, J. Am. Ceram. Soc. 85 (2002) 279–281.
[38] P. Pettersson, P. Johnsson, Z. Shen, Parameters for measuring the thermal shock of ceramic materials with an indentation-quench method, J. Eur. Ceram. Soc. 22 (2002) 1883–1889.
[39] A. Kovalčíková, J. Dusza, P. Šajgalík, Thermal shock resistance and fracture toughness of liquid-phase-sintered SiC-based ceramics, J. Eur. Ceram. Soc. 29 (2009) 2387–2394.
[40] S. Maensiri, S.G. Roberts, Thermal shock resistance of sintered alumina/silicon carbide nanocomposites evaluated by indentation techniques, J. Am. Ceram. Soc. 85 (2002) 1971–1978.
[41] Z. Kónya, I. Vesselényi, K. Niesz, A. Kukovecz, A. Demortier, A. Fonseca, J. Delhalle, Z. Mekhalif, J.B. Nagy, A.A. Koós, Z. Osváth, A. Kocsonya, L.P. Biró, I. Kiricsi, Large scale production of short functionalized carbon nanotubes, Chem. Phys. Lett. 360 (2002) 429–435.
[42] B.R. Lawn, Fracture of Brittle Solids, 2nd edition, Cambridge University Press, Cambridge, UK, 1993.
[43] G.A. Gogotsi, Fracture toughness of ceramics and ceramic composites, Ceram. Int. 29 (2003) 777–784.
[44] D.K. Shetty, I.G. Wright, P.N. Mincer, A.H. Clauser, Indentation fracture of WC-Co cermets, J. Mater. Sci. 20 (1985) 1873–1882.
[45] O. Koszor, A. Lindemann, F. Davin, C. Balazsi, Observation of thermophysical and tribological properties of CNT reinforced Si_3N_4, Key Eng. Mater. 409 (2009) 354–357.
[46] E.L. Corral, H. Wang, J. Garay, Z. Munir, E.V. Barrera, Effect of single-walled carbon nanotubes on thermal and electrical properties of silicon nitride processed using spark plasma sintering, J. Eur. Ceram. Soc. 31 (2011) 391–400.
[47] Cs. Balázsi, B. Fényi, N. Hegman, Zs. Köver, F. Wéber, Z. Vértesy, Z. Kónya, I. Kiricsi, L.P. Biró, P. Arató, Development of CNT/Si_3N_4 composites with improved mechanical and electrical properties, Compos. Part B 37 (2006) 418–424.
[48] S.-I. Shi, J. Liang, Effect of multiwall carbon nanotubes on electrical and dielectric properties of yttria-stabilized zirconia ceramic, J. Am. Ceram. Soc. 89 (2006) 3533–3535.